

Mass-Radius Relation for Rocky Planets based on PREM

Li Zeng^{1,a}, Dimitar Sasselov^{2,b}, and Stein Jacobsen^{1,c}

¹*Department of Earth and Planetary Sciences, Harvard University, Cambridge, MA 02138*

²*Astronomy Department, Harvard University, Cambridge, MA 02138*

^aastrozeng@gmail.com

^bdsasselov@cfa.harvard.edu

^cjacobsen@neodymium.harvard.edu

ABSTRACT

Several small dense exoplanets are now known, inviting comparisons to Earth and Venus. Such comparisons require translating their masses and sizes to composition models of evolved multi-layer-interior planets. Such theoretical models rely on our understanding of the Earth’s interior, as well as independently derived equations of state (EOS), but have so far not involved direct extrapolations from Earth’s seismic model -PREM. In order to facilitate more detailed compositional comparisons between small exoplanets and the Earth, we derive here a semi-empirical mass-radius relation for two-layer rocky planets based on PREM: $\frac{R}{R_{\oplus}} = (1.07 - 0.21 \cdot \text{CMF}) \cdot (\frac{M}{M_{\oplus}})^{1/3.7}$, where CMF stands for Core Mass Fraction. It is applicable to $1 \sim 8 M_{\oplus}$ and CMF of $0.0 \sim 0.4$. Applying this formula to Earth and Venus and several known small exoplanets with radii and masses measured to better than $\sim 30\%$ precision gives a CMF fit of 0.26 ± 0.07 .

Subject headings: Extrasolar planets, interiors, mass-radius relation, core mass fraction

1. Introduction

A first step in deriving the compositional diversity of small rocky planets was accomplished recently by (Dressing et al. 2015), who added Kepler-93b to the list of a dozen or so small exoplanets with radii and masses measured to better than $\sim 30\%$ precision. With exquisite sizes (mostly from Kepler light curves) and huge follow-up effort (Dressing et al. 2015; Pepe et al. 2013; Batalha et al. 2011; Ballard et al. 2013; Carter et al. 2012; Hatzes et al.

2011; Berta-Thompson et al. 2015) the mass-radius diagram is finally amenable to some detailed comparisons with theory in the 1 to 10 M_{\oplus} range. Closer to the mass and size of Earth, the rocky planets known to-date seem to exhibit an unexpectedly tight compositional correlation. Is this correlation really shared with Earth and Venus? If so, to what level of precision and under what assumptions? To begin answering such questions we must first acknowledge that models of the interior structure and composition of rocky exoplanets in the Super-Earth domain are based largely on experience (and extrapolations) from the models of the rocky solar system planets, and mostly - the Earth (Valencia et al. 2006, 2007b,a; Fortney et al. 2007; Seager et al. 2007; Zeng & Seager 2008; Grasset et al. 2009; Zeng & Sasselov 2013). Here instead of using simple shell models based on EOSs of minerals and metals, we take a different approach and derive semi-empirical EOSs based on the well-constrained seismic model of the Earth.

2. Equation of State (EOS)

On one hand, in several previous models of solid exoplanets (Zeng & Sasselov 2013; Zeng & Seager 2008; Seager et al. 2007), cores and mantles of solid exoplanets are modeled as pure ϵ -Fe-solid and Mg-perovskite/post-perovskite respectively. On the other hand, we know the actual density variation inside Earth through measurements of seismic wave velocities. This seismically derived density model is widely known as PREM (Preliminary Reference Earth Model (Dziewonski & Anderson 1981)). The differences between the two approaches, primarily (1) the liquid outer core less dense than pure ϵ -Fe solid and (2) the upper mantle less dense than the extrapolation of lower mantle, can cause differences in the mass-radius relations derived.

There are several assumptions made when we extrapolate PREM. We assume the upper mantle to lower mantle phase transition occurs at the same pressure as the Earth’s interior. It is a pressure-driven phase transition, so temperature effect is secondary and thus ignored.

The Thomas-Fermi-Dirac Model modified with Correlation Energy (Salpeter & Zapolsky 1967) (abbreviated as TFD from now on) serves as a lower bound for the density of material considered. Any properly-behaving EOS should asymptotically approach TFD above ~ 1 TPa, as at such high pressures the electron degeneracy pressure dominates while the detailed chemical and crystal structures of the material become less important.

We will show that the Birch-Murnaghan 2nd order EOS (abbreviated as BM2 from now on) (Birch 1952) provides a fairly decent description of how material is compressed in Earth’s interior for both core (good up to 12 TPa where it asymptotically approaches TFD)

and mantle (good up to 3.5 TPa where it asymptotically approaches TFD). Those pressures roughly correspond to the central pressure and core-mantle boundary pressure respectively of a $30 M_{\oplus}$ rocky planet with CMF=0.3.

$$P = \frac{3}{2} \cdot K_0 \left[\left(\frac{\rho}{\rho_0} \right)^{\frac{7}{3}} - \left(\frac{\rho}{\rho_0} \right)^{\frac{5}{3}} \right] \quad (1)$$

The fit to lower mantle, outer core and inner core PREM gives:

- Lower Mantle: $\rho_0 = 3.98$ g/cc, $K_0 = 206$ GPa, error $\sim 1\%$ in ρ .
- Outer Core: $\rho_0 = 7.05$ g/cc, $K_0 = 201$ GPa, error $\sim 1\%$ in ρ .
- Inner Core: $\rho_0 = 7.85$ g/cc, $K_0 = 255$ GPa, error $\sim 0.01\%$ in ρ .

The uncertainties of the fit are similar to the intrinsic uncertainty of PREM in ρ of $\sim 1\%$ (See (Ricolleau et al. 2009) and (Ritsema et al. 2011) and Figure 3 of (Huang et al. 2011)).

2.1. PREM-extrapolated EOS for Mantle

Inside Earth, the density jump from upper mantle to lower mantle is 10% from 4 g/cc to 4.4 g/cc at 23.83 GPa. Earth’s upper mantle consists of complex phases of Mg-silicates, including various polymorphs of olivine: (α) olivine, (β) wadsleyite, and (γ) ringwoodite (Bina 2003). The upper mantle to lower mantle transition occurs at 670 km depth in Earth (about 10.5% Earth radius). For more massive planets like Kepler-93b, this transition occurs at shallower depth ($\sim 3\%$ radius of Kepler-93b) for the same pressure.

Fig. 1 shows the comparison of different EOS of Mg-silicates.

Interestingly, the TFD beyond 1 TPa for MgO, SiO₂, MgSiO₃, and Mg₂SiO₄ are almost identical as they all have average atomic weight A=20 and average atomic charge Z=10. This coincidence simplifies the EOS of Mg-silicates, as it indicates that Mg/Si ratio does not matter towards the high-pressure end. It only matters towards the low-pressure end, which is captured in our EOS by using the PREM density variation in the upper-mantle pressure range.

According to Fig. 1, except the prominent density jump of 10% at the upper-lower mantle boundary, the other high-pressure phase transitions are only $\sim 1\%$ level in density and thus insignificant in mass-radius calculation (Unterborn et al. 2015). Therefore, in this paper we adopt the EOS of Mg-silicates mantle as follows:

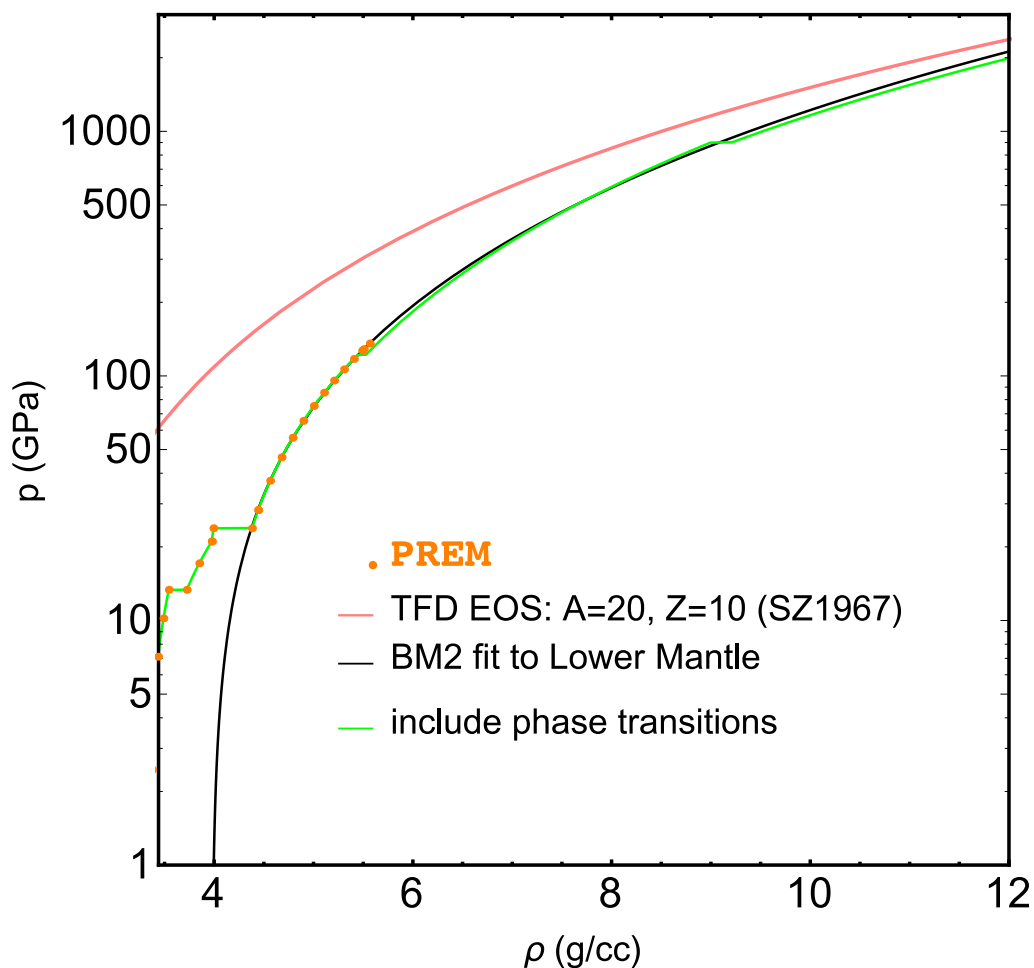


Fig. 1.— Orange points: PREM density of Earth’s mantle, excerpt from Appendix G of (Stacey & Davis 2008). Pink curve: TFD for $A=20$ and $Z=10$. Black curve: BM2 fit to lower-mantle PREM ($\rho_0 = 3.98$ g/cc, $K_0 = 206$ GPa). Green curve: including lower-mantle phase transitions and pv-ppv phase transition at 122 GPa (Zeng & Sasselov 2013; Caracas & Cohen 2008; Spera et al. 2006) and further dissociation of ppv at 0.9 and 2.1 TPa (Umemoto & Wentzcovitch 2011; Wu et al. 2011).

- 0 GPa - 23.83 GPa: linear interpolation of the lower mantle density according to the Appendix G of (Stacey & Davis 2008), which is taken from PREM. i.e. follow the green curve in Fig. 1.
- 23.83 GPa - 3.5 TPa: BM2 EOS with $\rho_0 = 3.98$ g/cc, $K_0 = 206$ GPa, (error $\sim 1\%$ in density). i.e. follow the black curve in Fig. 1.
- >3.5 TPa: TFD EOS of MgSiO_3 calculated using method in (Salpeter & Zapolsky 1967). i.e. follow the pink curve in Fig. 1.

2.2. PREM-extrapolated EOS for Core

Fig. 2 shows the comparison of different EOS of the Core.

In Earth, the density jump from liquid outer core to solid inner core is 5% from 12.2 g/cc to 12.8 g/cc at 328.85 GPa. The Rydberg EOS of pure solid ϵ -Fe phase, which is experimentally determined from static compression up to 205 GPa (Dewaele et al. 2006; Wagner et al. 2012), is too high of density (cyan curve in Fig. 2) in the pressure region relevant to Earth, even including the temperature effect (green curve in Fig. 2), even for the solid inner core. This is likely due to the presence of several weight percent of one or more light elements (McDonough 2014). The lighter elements could be S, Si, O, C, or a combination of them (Badro et al. 2007; Fischer et al. 2012; Alfè et al. 2002; Poirier 1994; Stixrude et al. 1997; Anderson & Ahrens 1994), but no agreement is reached as to which of these elements are most important. The Rydberg EOS with or without temperature behaves poorly for extrapolation above ~ 1 TPa as it overshoots and crosses over the TFD EOS, which serves as a lower bound for the density of Fe.

As such, we choose to only extrapolate the liquid outer core BM2 EOS to higher pressure until it asymptotically approaches the TFD EOS. The solid inner core is likely a secondary feature resulting from the crystallization of the liquid core. It currently comprises only a small fraction ($\approx 3\%$) of the total mass of the Earth, and in more massive planets, the focus of this study, solid inner core may not exist at all due to higher heat content and slower cooling rate. BM2 EOS behaves nicely as it asymptotically approaches the TFD EOS at vert high pressure (~ 12 TPa).

Therefore, in this paper we adopt the EOS of Fe core as follows:

- 0 GPa - 12 TPa: BM2 EOS with $\rho_0 = 7.05$ g/cc, $K_0 = 201$ GPa, (error $\sim 1\%$ in density). i.e. follow the black curve in Fig. 2.

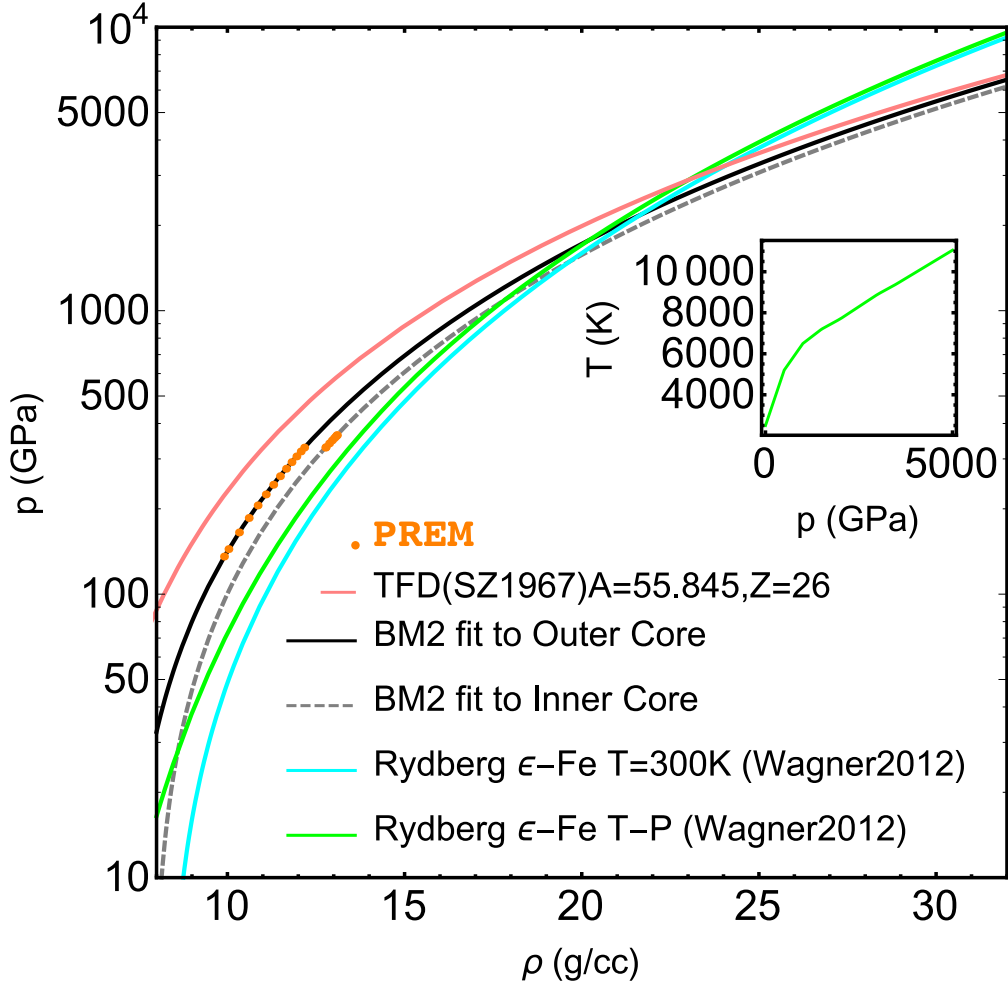


Fig. 2.— Orange points: PREM density of Earth's core, excerpt from Appendix G of (Stacey & Davis 2008). Pink curve: TFD of iron ($A=55.845$ and $Z=26$). Black curve: BM2 fit to outer-core PREM ($\rho_0 = 7.05$ g/cc, $K_0 = 201$ GPa). Gray dashed curve: BM2 fit to inner-core PREM ($\rho_0 = 7.85$ g/cc, $K_0 = 255$ GPa). Cyan curve: Rydberg ϵ -Fe EOS at 300K isotherm according to (Dewaele et al. 2006). Green curve: Rydberg ϵ -Fe EOS (Dewaele et al. 2006) with T-P profile (small inset plot) of rocky planet core interpolated from Wagner et al. (2012).

- >12 TPa: TFD EOS of Fe (A=55.845 and Z=26) calculated using method in (Salpeter & Zapolsky 1967). i.e. follow the pink curve in Fig. 2.

3. Mass-Radius Relation

Dressing et al. (2015) points out a tight mass-radius relation of solid exoplanets between 2 and 5 M_{\oplus} from the comparison of Earth, Venus, and several dense exoplanets by using the mass-radius contours described in (Zeng & Sasselov 2013). However, Dressing et al. (2015)'s CMF fit of 17% is much lower than that of Earth or Venus. Here we show that using the PREM-extrapolated EOS renders a better fit of CMF in agreement with that of Earth and Venus (See Fig. 3).

There might be a selection bias towards higher density planets by selecting only the planets with better than $\sim 30\%$ mass measurement accuracy. However, as already pointed out by Dressing et al. (2015), the low mass planets with very low densities like Kepler-11b and Kepler-138d do not detract from the conclusion that all the rocky analogs of the Earth obey a single mass-radius relation. The degree to which this is true will be tested by more precise mass measurements.

The planets in Fig. 3 are tabulated in Table 1.

Table 1: CMF of Planets

Planet	$M(M_{\oplus})$	$R(R_{\oplus})$	CMF
Earth ¹	1	1	0.325 ± 0.001
Venus ¹	0.815	0.9499	0.31 ± 0.01
K-10b	3.33 ± 0.49 (Dumusque et al. 2014)	$1.47^{+0.03}_{-0.02}$ (Dumusque et al. 2014)	0.04 ± 0.2
K-36b	$4.45^{+0.33}_{-0.27}$ (Carter et al. 2012)	1.486 ± 0.035 (Carter et al. 2012)	0.37 ± 0.14
K-78b	$1.86^{+0.38}_{-0.25}$ (Pepe et al. 2013)	$1.173^{+0.159}_{-0.089}$ (Pepe et al. 2013)	$0.37^{+0.3}_{-0.5}$
K-93b	4.02 ± 0.68 (Dressing et al. 2015)	1.478 ± 0.019 (Ballard et al. 2013)	0.26 ± 0.2
COROT-7b	5.74 ± 0.86 (Haywood et al. 2014)	1.585 ± 0.064 (Barros et al. 2014)	0.14 ± 0.3
HD219134b	4.46 ± 0.47 (Motalebi et al. 2015)	1.606 ± 0.086 (Motalebi et al. 2015)	0.0 ± 0.3
GJ1132b	1.62 ± 0.55 (Berta-Thompson et al. 2015)	1.16 ± 0.11 (Berta-Thompson et al. 2015)	0.25 ± 0.5

The mass-radius curves in Fig. 3 are tabulated in Table 2.

¹In the calculation, we treat the errors in CMF of Earth and Venus as ± 0.2 , comparable to the errors for exoplanets considered here, so as not to bias the fit.

²mass in Earth Mass ($M_{\oplus} = 5.9742 \times 10^{24} kg$)

³radius in Earth Radius ($R_{\oplus} = 6.371 \times 10^6 m$)

Table 2: Mass-Radius Table

	100%fe	50%fe	30%fe	25%fe	20%fe	rock	25%h2o	50%h2o	100%h2o
$M(M_{\oplus})^2$	$R(R_{\oplus})^3$	$R(R_{\oplus})$	$R(R_{\oplus})$	$R(R_{\oplus})$	$R(R_{\oplus})$	$R(R_{\oplus})$	$R(R_{\oplus})$	$R(R_{\oplus})$	$R(R_{\oplus})$
0.125	0.445	0.523	0.547	0.553	0.558	0.58	0.649	0.697	0.776
0.25	0.55	0.645	0.672	0.679	0.685	0.711	0.793	0.851	0.952
0.5	0.676	0.789	0.823	0.832	0.84	0.872	0.969	1.039	1.163
1	0.823	0.961	1.005	1.016	1.026	1.067	1.182	1.27	1.41
2	0.99	1.164	1.22	1.23	1.25	1.3	1.44	1.54	1.71
4	1.176	1.4	1.47	1.49	1.5	1.57	1.74	1.85	2.05
8	1.38	1.66	1.75	1.77	1.79	1.88	2.07	2.21	2.45
16	1.59	1.94	2.06	2.08	2.11	2.22	2.45	2.61	2.9
32	1.82	2.25	2.38	2.42	2.45	2.58	2.85	3.04	3.36

3.1. Mass-Radius Formula Fitting for Rocky Planets

The CMF-dependent mass-radius relation of rocky planets can be fit to the following formula (for $0 \leq \text{CMF} \leq 0.4$, $1M_{\oplus} \leq M \leq 8M_{\oplus}$). It agrees with the actual mass-radius curves in Fig. 3 within $\sim 0.01 R_{\oplus}$ in radius. If we use it to calculate CMF, it gives an uncertainty of ~ 0.02 in CMF.

$$\left(\frac{R}{R_{\oplus}}\right) = (1.07 - 0.21 \cdot \text{CMF}) \left(\frac{M}{M_{\oplus}}\right)^{1/3.7} \quad (2)$$

Eq. 2 can be inverted to solve for CMF given the mass and radius:

$$\text{CMF} = \frac{1}{0.21} [1.07 - (\frac{R}{R_{\oplus}}) / (\frac{M}{M_{\oplus}})^{1/3.7}] \quad (3)$$

For comparison, this semi-empirical mass-radius formula is in agreement with the mass-radius relation of super-Earths presented in Valencia et al. (2006), which is a scaling law of $R \propto M^{0.267-0.272}$. This new formula takes one step further to articulate the dependence on CMF, which is useful in differentiating among rocky planets with different CMF (i.e. compositions).

For Earth, $\text{CMF}_{\oplus} = \frac{1}{0.21} [1.07 - (1)/(1)^{1/3.7}] = 0.07/0.21 = 0.33$. For Kepler-93b, $\text{CMF}_{K93b} = \frac{1}{0.21} [1.07 - (1.478)/(4.02)^{1/3.7}] = 0.26$. The uncertainties (δCMF) in CMF resulting from the uncertainties in mass and radius can be derived from Eq. 3:

$$|\delta\text{CMF}| \approx 5 \times \sqrt{\left|\frac{\delta r}{r}\right|^2 + \left(\frac{1}{3.7}\right)^2 \left|\frac{\delta m}{m}\right|^2} \quad (4)$$

So in order to tell a 20% core mass apart from a 30% core mass, radius needs to be measured to better than 2% level, or equivalently, mass to 6% level. For Kepler-93b, $|\frac{\delta r}{r}| = \frac{0.019}{1.478} = 0.013$ and $|\frac{\delta m}{m}| = \frac{0.68}{4.02} = 0.17$, so $|\delta\text{CMF}| = 0.2$. Therefore, $\text{CMF}_{K93b} = 0.26 \pm 0.2$. Table 1 Column 4 lists the CMF estimates of these exoplanets.

Assuming this population of dense exoplanets follows the same CMF distribution, we then apply a weighted least-square fit to Table 1.

Denote the weighted average of CMF as $\overline{\text{CMF}}$:

$$\overline{\text{CMF}} = \frac{\sum_i \left(\frac{\text{CMF}}{\delta\text{CMF}^2}\right)}{\sum_i \left(\frac{1}{\delta\text{CMF}^2}\right)} \quad (5)$$

Denote the standard deviation of CMF as σCMF :

$$\sigma\text{CMF} = \sqrt{1 / \left(\sum_i \frac{1}{\delta\text{CMF}^2}\right)} \quad (6)$$

Result: $\overline{\text{CMF}} = 0.26$ and $\sigma\text{CMF} = 0.07$, indicating Earth-like composition (CMF ~ 0.3) carries on up to at least $\sim 5 M_{\oplus}$.

3.2. Discussion

This is backed up by recent studies of disintegrated planet debris in polluted white dwarf spectra (Jura & Young 2014; Wilson et al. 2015; Xu et al. 2014). These studies show that the accreted extrasolar planet debris generally resemble bulk Earth composition ($> 85\%$ by mass composed of O, Mg, Si, Fe), similar Fe/Si and Mg/Si ratio and are carbon-poor. It indicates formation processes similar to those controlling the formation and evolution of objects in the inner solar system (Jura & Young 2014).

In our solar system, evidence suggests that rocky bodies were formed from chondritic-like materials (cf. Lodders & Fegley 2010). Current planet formation theory suggests that the solar nebula was initially heated to very high temperatures to the extent that virtually everything was vaporized except for small amount of presolar grains (Ott 2007). The

nebula then cools to condense out various elements and mineral assemblages from the vapor phase at different temperatures according to the condensation sequence (White 2013). Fe-Ni metal alloy and Mg-silicates condense out around similar temperatures of 1200-1400K (depending on the pressure of the nebula gas) according to thermodynamic condensation calculation (Lodders 2003). Oxygen, on the other hand, does not have a narrow condensation temperature range, as it is very abundant and it readily combines with all kinds of metals to form oxides which condense out at various temperatures as well as H, N, C to form ices condensing out at relatively low temperatures (Lewis 1997). As supported by the polluted white dwarf study, we expect other exoplanetary systems to follow similar condensation sequence as the solar system in a H-dominated nebular environment for the major elements: Fe, Mg, Si, and O (Jura & Young 2014).

In solar system, the primitive CI Carbonaceous Chondrites have Fe : Mg : Si = 0.855 : 1.047 : 1 (McDonough & Sun 1995). If all this Fe forms the core, $CMF \approx 0.38$ is the upper limit. If some Fe is incorporated into the mantle either as metal or oxides, CMF becomes less. The solar ratio of Fe/Si is representative for the stars in the solar neighborhood, which is a tight distribution centered at 1, while the Mg/Si=1 seems to tend towards the lower end of the distribution centered at 1.34 (Gilli et al. 2006; Grasset et al. 2009). A Mg/Si ratio higher than 1 could produce more olivine (Mg_2SiO_4) or more MgO to affect the mineralogy of the upper mantle (Bond et al. 2010; Delgado Mena et al. 2010; Pagano et al. 2015). However, it does not affect high-pressure EOS much. As we have pointed out earlier in Section 2 of EOS, the TFD EOS of MgO, SiO_2 , $MgSiO_3$, Mg_2SiO_4 will converge above ~ 1 TPa due to their identical average atomic weight of 20 and atomic charge of 10. Therefore, for more massive planets the effect of Mg/Si tends to be smaller. The dispersion expected from the variation in Mg/Si and Fe/Si ratios cause approximately 2% difference in radius (Grasset et al. 2009; Dressing et al. 2015).

Oxygen is more readily available than Fe, Mg, or Si (Lodders 2003), as it is richly produced in nuclear synthesis of massive stars and chemical evolution of Galaxy (Pagel 1997). So there is usually enough O to combine with Mg and Si to form Mg-silicates as well as to oxidize some Fe-metal. Comparing bodies in our solar system: the core mass fractions of Earth and Venus (Rubie et al. 2007) are around 0.3, the core mass fraction of Mars is estimated to be 0.2 (McSween 2003), and of Vesta is smaller, about 0.17 (Ermakov et al. 2014; Ruzicka et al. 1997). For asteroid parent bodies of iron meteorites, their core mass fractions are even smaller (Petaev & Jacobsen 2004). As such, there seems to exist a trend of increasing CMF from smaller objects towards bigger objects in the solar system. This trend seems to turn flat around $1 M_{\oplus}$.

These dense exoplanets between 2 and $5 M_{\oplus}$ so far appear to agree with the mass-

radius relation with $\text{CMF} \approx 0.26$, suggesting that they are like the Earth in terms of their proportions of mantle and core. But their surface conditions are utterly different as they are much too hot. This is due to observational bias that currently it is much easier for us to detect close-in planets around stars. The fact that we now see so many of them suggests there may be abundant Earth-like analogs at proper distances from their stars to allow existence of liquid water on their surfaces.

4. Summary

This paper provides a new CMF-dependent semi-empirical mass-radius relation for rocky planets of $0 \leq \text{CMF} \leq 0.4$ and $1M_{\oplus} \leq M \leq 8M_{\oplus}$.

The result of fit to several dense exoplanets: $\text{CMF} \approx 0.26 \pm 0.07$, agrees with the studies of disintegrated planet debris in polluted white dwarf spectra, the solar system formation theory and geochemical and cosmochemical evidence of meteorites.

The model tool is accessible at www.astrozeng.com.

5. Acknowledgement

The author Li Zeng is grateful to Simons Foundation for supporting his postdoctoral research position under the Simons Collaboration on the Origins of Life. The author Li Zeng would like to thank Courtney Dressing, Lars Buchhave, and Eugenia Hyung for inspiring discussions. Part of this research was conducted under the Sandia Z Fundamental Science Program and supported by the Department of Energy National Nuclear Security Administration under Award Number DE-NA0001804 to S. B. Jacobsen (PI) with Harvard University. This research is the authors' views and not those of the DOE.

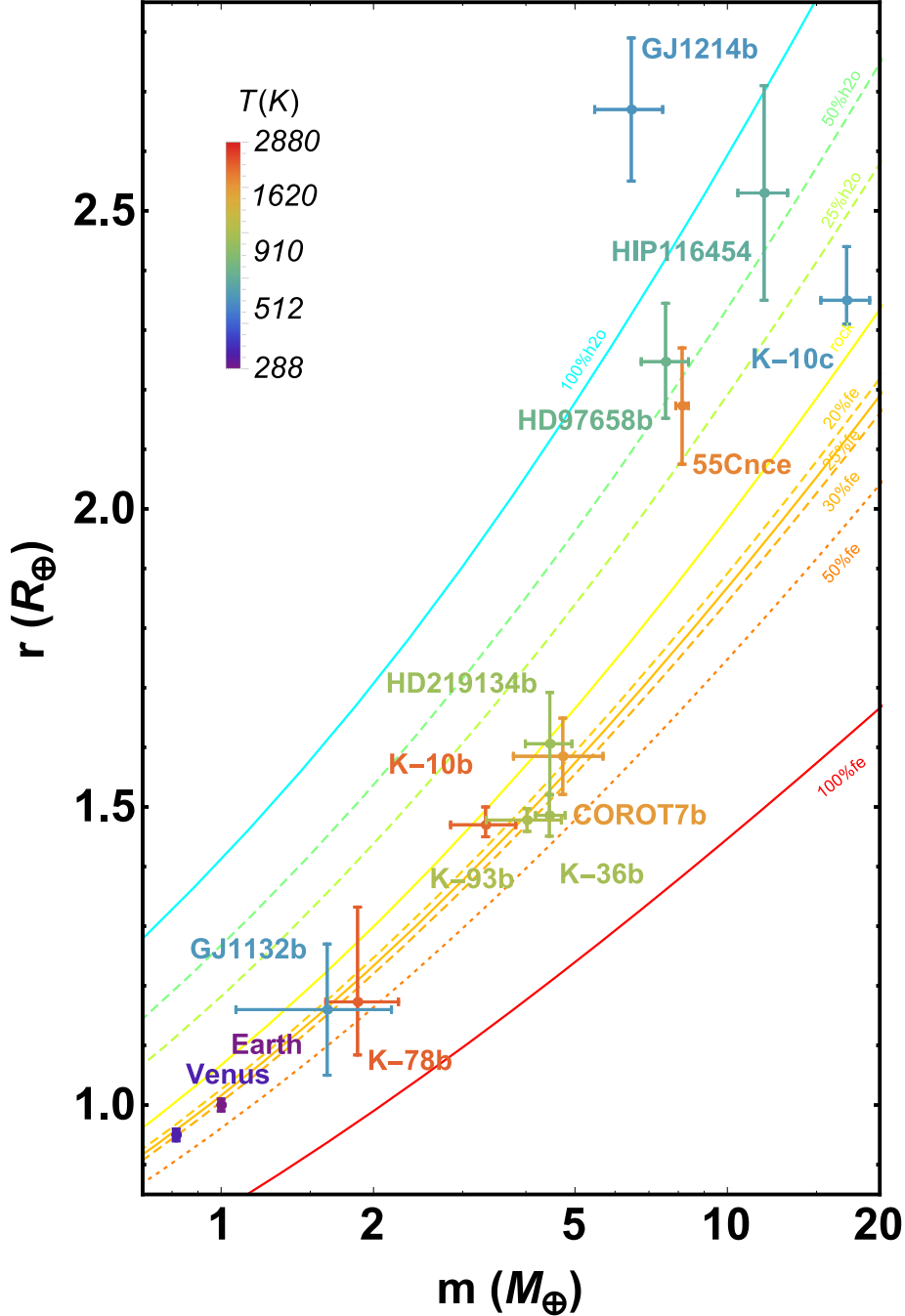


Fig. 3.— Mass-radius curves with planets color-coded by their surface temperatures (calculated from the stellar flux they receive assuming similar bond albedo as the Earth (≈ 0.3) and perfect heat redistribution). (Pepe et al. 2013; Dumusque et al. 2014; Dressing et al. 2015; Ballard et al. 2013; Carter et al. 2012; Haywood et al. 2014; Barros et al. 2014; Dragomir et al. 2013; Nelson et al. 2014; Winn et al. 2011; Vanderburg et al. 2015; Cochran et al. 2011; Charbonneau et al. 2009; Motalebi et al. 2015; Berta-Thompson et al. 2015)

REFERENCES

- Alfè, D., Gillan, M. J., & Price, G. D. 2002, *Earth and Planetary Science Letters*, 195, 91
- Anderson, W. W., & Ahrens, T. J. 1994, *J. Geophys. Res.*, 99, 4273
- Badro, J., Fiquet, G., Guyot, F., et al. 2007, *Earth and Planetary Science Letters*, 254, 233
- Ballard, S., Huber, D., Chaplin, W., et al. 2013, *ApJ*, submitted
- Barros, S. C. C., Almenara, J. M., Deleuil, M., et al. 2014, *A&A*, 569, A74
- Batalha, N. M., Borucki, W. J., Bryson, S. T., et al. 2011, *The Astrophysical Journal*, 729, 27
- Berta-Thompson, Z. K., Irwin, J., Charbonneau, D., et al. 2015, *Nature*, 527, 204
- Bina, C. R. 2003, *Treatise on Geochemistry*, 2, 39
- Birch, F. 1952, *J. Geophys. Res.*, 57, 227
- Bond, J. C., O’Brien, D. P., & Laretta, D. S. 2010, *ApJ*, 715, 1050
- Caracas, R., & Cohen, R. E. 2008, *Physics of the Earth and Planetary Interiors*, 168, 147
- Carter, J. A., Agol, E., Chaplin, W. J., et al. 2012, *Science*, 337, 556
- Charbonneau, D., Berta, Z. K., Irwin, J., et al. 2009, *Nature*, 462, 891
- Cochran, W. D., Fabrycky, D. C., Torres, G., et al. 2011, *The Astrophysical Journal Supplement Series*, 197, 7
- Delgado Mena, E., Israelian, G., González Hernández, J. I., et al. 2010, *ApJ*, 725, 2349
- Dewaele, A., Loubeyre, P., Occelli, F., et al. 2006, *Physical Review Letters*, 97, doi:10.1103/physrevlett.97.215504
- Dragomir, D., Matthews, J. M., Eastman, J. D., et al. 2013, *ApJ*, 772, L2
- Dressing, C. D., Charbonneau, D., Dumusque, X., et al. 2015, *ApJ*, 800, 135
- Dumusque, X., Bonomo, A. S., Haywood, R. D., et al. 2014, *ApJ*, 789, 154
- Dziewonski, A. M., & Anderson, D. L. 1981, *Physics of the Earth and Planetary Interiors*, 25, 297

- Ermakov, A. I., Zuber, M. T., Smith, D. E., et al. 2014, *Icarus*, 240, 146
- Fischer, R. A., Campbell, A. J., Caracas, R., et al. 2012, *Earth and Planetary Science Letters*, 357, 268
- Fortney, J., Marley, M., & Barnes, J. 2007, *The Astrophysical Journal*, 659, 1661
- Gilli, G., Israelian, G., Ecuivillon, A., Santos, N. C., & Mayor, M. 2006, *A&A*, 449, 723
- Grasset, O., Schneider, J., & Sotin, C. 2009, *The Astrophysical Journal*, 693, 722
- Hatzes, A. P., Fridlund, M., Nachmani, G., et al. 2011, *The Astrophysical Journal*, 743, 75
- Haywood, R. D., Collier Cameron, A., Queloz, D., et al. 2014, *MNRAS*, 443, 2517
- Huang, H., Fei, Y., Cai, L., et al. 2011, *Nature*, 479, 513
- Jura, M., & Young, E. D. 2014, *Annual Review of Earth and Planetary Sciences*, 42, 45
- Lewis, J. S. 1997, *Physics and chemistry of the solar system*
- Lodders, K. 2003, *ApJ*, 591, 1220
- Lodders, K., & Fegley, B. 2010, *Chemistry of the Solar System: RSC (RSC Paperbacks)* (Royal Society of Chemistry)
- McDonough, W. 2014, in *Treatise on Geochemistry (Second Edition)*, second edition edn., ed. H. D. H. K. Turekian (Oxford: Elsevier), 559 – 577
- McDonough, W., & Sun, S. 1995, *Chemical Geology*, 120, 223 , *chemical Evolution of the Mantle*
- McSween, Jr., H. Y. 2003, *Treatise on Geochemistry*, 1, 601
- Motalebi, F., Udry, S., Gillon, M., et al. 2015, *ArXiv e-prints*, arXiv:1507.08532
- Nelson, B. E., Ford, E. B., Wright, J. T., et al. 2014, *MNRAS*, 441, 442
- Ott, U. 2007, *Presolar Grains in Meteorites and Their Compositions*, ed. R. von Steiger, G. Gloeckler, & G. M. Mason (Springer Science+Business Media), 87
- Pagano, M., Truitt, A., Young, P. A., & Shim, S.-H. 2015, *ApJ*, 803, 90
- Pagel, B. E. J. 1997, *Nucleosynthesis and Chemical Evolution of Galaxies*
- Pepe, F., Collier Cameron, A., Latham, D. W., et al. 2013, *ArXiv e-prints*, arXiv:1310.7987

- Petaev, M. I., & Jacobsen, S. B. 2004, *Meteoritics and Planetary Science*, 39, 1685
- Poirier, J.-P. 1994, *Physics of the Earth and Planetary Interiors*, 85, 319
- Ricolleau, A., Fei, Y., Cottrell, E., et al. 2009, *Geophys. Res. Lett.*, 36, L06302
- Ritsema, J., Deuss, A., van Heijst, H. J., & Woodhouse, J. H. 2011, *Geophysical Journal International*, 184, 1223
- Rubie, D., Nimmo, F., & Melosh, H. 2007, in *Treatise on Geophysics*, ed. G. Schubert (Amsterdam: Elsevier), 51 – 90
- Ruzicka, A., Snyder, G. A., & Taylor, L. A. 1997, *Meteoritics and Planetary Science*, 32, 825
- Salpeter, E. E., & Zapolsky, H. S. 1967, *Physical Review*, 158, 876
- Seager, S., Kuchner, M., Hier-Majumder, C. A., & Militzer, B. 2007, *The Astrophysical Journal*, 669, 1279
- Spera, F. J., Yuen, D. A., & Giles, G. 2006, *Physics of the Earth and Planetary Interiors*, 159, 234
- Stacey, F. D., & Davis, P. M. 2008
- Stixrude, L., Wasserman, E., & Cohen, R. E. 1997, *J. Geophys. Res.*, 102, 24729
- Umemoto, K., & Wentzcovitch, R. M. 2011, *Earth and Planetary Science Letters*, 311, 225
- Unterborn, C. T., Dismukes, E. E., & Panero, W. R. 2015, ArXiv e-prints, arXiv:1510.07582
- Valencia, D., O’Connell, R. J., & Sasselov, D. 2006, *Icarus*, 181, 545
- Valencia, D., Sasselov, D. D., & O’Connell, R. J. 2007a, *The Astrophysical Journal*, 665, 1413
- . 2007b, *The Astrophysical Journal*, 656, 545
- Vanderburg, A., Montet, B. T., Johnson, J. A., et al. 2015, *ApJ*, 800, 59
- Wagner, F. W., Tosi, N., Sohl, F., Rauer, H., & Spohn, T. 2012, *A&A*, 541, A103
- White, W. M. 2013, *Geochemistry* (Wiley-Blackwell)
- Wilson, D. J., Gänsicke, B. T., Koester, D., et al. 2015, *MNRAS*, 451, 3237
- Winn, J. N., Matthews, J. M., Dawson, R. I., et al. 2011, *ApJ*, 737, L18

Wu, S., Umemoto, K., Ji, M., et al. 2011, *Phys. Rev. B*, 83, 184102

Xu, S., Jura, M., Koester, D., Klein, B., & Zuckerman, B. 2014, *ApJ*, 783, 79

Zeng, L., & Sasselov, D. 2013, *Publications of the Astronomical Society of the Pacific*, 125, pp. 227

Zeng, L., & Seager, S. 2008, *Publications of the Astronomical Society of the Pacific*, 120, 983